Journal of Materials Chemistry

Cite this: *J. Mater. Chem.*, 2011, **21**, 4416

www.rsc.org/materials

PAPER

Multi-responsive polymer nanoparticles from the amphiphilic poly(dimethylsiloxane) (PDMS)-containing poly(ether amine) (PDMS-gPEA) and its potential application for smart separation†

Chunfeng Di, Xuesong Jiang,* Rui Wang and Jie Yin

Received 21st October 2010, Accepted 17th December 2010
DOI: 10.1039/c0jm03569f

We report here a novel amphiphilic PDMS-containing poly(ether amine) (PDMS-gPEA) synthesized through one-pot condensation polymerization of commercial di-epoxy and amine monomers. The obtained PDMS-gPEA could be dispersed directly in aqueous solution to form stable uniform-sized nanoparticles with a diameter of about 16 nm, whose aggregation is responsive to temperature, pH and ionic strength with tunable cloud point (CP). The whole process for the responsive aggregation of PDMS-gPEA nanoparticles was revealed by transmission electron microscope (TEM) and dynamic light scattering (DLS), and was intensively studied by UV-vis spectra. The responsive nanoparticles of PDMS-gPEA possessed the unique selective encapsulation of water-soluble dye, which provides potential applications in smart separations.

1. Introduction

Due to their potential applications in separations, biosensors, chemical storage and transport and gene and drug delivery, polymer nanoparticles that respond to environmental stimuli have attracted much attention.[1–6] The stimuli-responsive behaviors of polymer nanoparticles strongly depend on the external chemical and physical stimuli, such as ionic strength, light, electric and magnetic fields, temperature and pH.[7–9] As the change in behavior of responsive polymer nanoparticles is often a result of their response to a combination of environmental changes in nature, polymer nanoparticles which are sensitive to temperature, pH and ionic strength simultaneously are very important in practical applications, and hence are of significant interest.[6,10–18]

Generally, responsive polymer nanoparticles are fabricated by self-assembly of amphiphilic double or tri- block polymers, which contain at least one block that is responsive to external stimuli.[19–27] Therefore, synthesis of amphiphilic block polymers with a designed structure is one of the key factors in fabrication of responsive polymer nanoparticles. Usually, these block polymers are synthesized through living polymerization or chain propagation such as ring-opening polymerization (ROP),[28,29] atom transfer radical polymerization (ATRP)[30,31] and reversible addition fragmentation chain-transfer (RAFT) polymerization.[6,32,33] Although various block polymers comprising responsive blocks such as PNIPAM and PEGMA have been reported,[34–37] it is still difficult to obtain these block polymers by industrial large-scale production due to some extreme reaction conditions and time-consuming post-processing of these living polymerizations, which consequently limits the application of responsive polymer micelles to a certain extent. Therefore, the main challenge for responsive polymer nanoparticles is low-cost synthesis of inexpensive amphiphilic polymers, which can construct multi-responsive polymer nanoparticles through a very robust and simple approach.[38] In some applications such as separations, water-treatment and in pharmaceutical industries, these amphiphilic polymers should compete with surfactants. In this case, the cost of synthesis of amphiphilic polymers will indeed play a key role. Recently, we developed a novel family of amphiphilic poly(ether amine)s (PEAs), which could be obtained through one-pot synthesis of condensation polymerization of commercial di-epoxy and amine monomers. These PEAs could be dispersed directly in water to form polymer nanoparticles, which were multi-responsive to temperature, pH and ionic concentration.[39,40]

Motivated by the novel characteristics of PEA such as easy synthesis, low-cost, robust and simple approach to formation of multi-responsive polymer nanoparticles, we continued to synthesize graft poly(ether amine) containing a poly(dimethylsiloxane) (PDMS) short chain in the backbone. As an inorganic polymeric chain, PDMS is of interest because of its excellent hydrophobic ability, and chemical and thermo stability.[41,42] The multi-responsive behavior of polymer nanoparticles formed by PDMS-gPEA, as well as their application in the controlled and reversible separation of dyes was investigated.

School of Chemistry & Chemical Technology, State Key Laboratory for Metal Matrix Composite Materials, Shanghai Jiao Tong University, Shanghai, China. E-mail: ponygle@sjtu.edu.cn; Fax: +86-21-54747445; Tel: +86-21-54743268

† Electronic supplementary information (ESI) available. See DOI: 10.1039/c0jm03569f

It is interesting that PDMS-gPEA nanoparticles can adsorb water-soluble dyes with unique selectivity, which provides potential applications in smart separations.

2. Experimental section

2.1. Materials

Poly(propylene glycol) diglycidyl ether (PPO-DE, Aldrich, M_n = 640 g mol^{-1}), Jeffamine L100 (Huntsman, M_n= 1000 g mol^{-1}), ethanol absolute (Sinopharm Chemical, >99.7 %), poly(dimethylsiloxane), diglycidyl ether (PDMS-DE, Aldrich, M_n = 980 g mol^{-1}), cellulose dialysis membrane (Shanghai Greenbird Tech. Co. Ltd., Cut-off M_w = 3500), methyl orange (Sinopharm Chemical), calcein (Sinopharm Chemical, AR), Rose Bengal sodium salt (Sinopharm Chemical, BR), Rhodamine 6G (Sigma) were used as received.

2.2. Synthesis of PDMS-gPEA

PDMS-gPEA was synthesized through one-step according to our previous report.[40] The reaction was conducted in a 50 mL two-neck flask equipped with a nitrogen inlet tube and a reflux condenser. The mixture of L100 (0.006 mol), PDMS-DE (0.003 mol), PPO-DE (0.003 mol) and 50 ml ethanol was refluxed for 24 h under protection of nitrogen. After cooling to room temperature, the mixture was moved into a dialysis bag to dialyze in ethanol for 3 days. Then the ethanol was removed using rotary evaporation leaving the product. $M_n = 9.1 \times 10^3$, $M_w/M_n = 1.55$ (determined using DMF as eluent). ^{1}H NMR ($CDCl_3$,400 MHz): δ = 3.71–3.32 (–OCH_3, OCH_2 and OCH), 2.54–2.83 (–NCH_2), 1.13, 0.49 and 0.09 (CH_3 and CH_2); FTIR (KBr): 3400 (O–H), 2864 (C–H), 1086 (C–O–C) and 1020 cm^{-1} (Si–O).

2.3. Separation of dye

Dye and PDMS-gPEA were dissolved in water together (0.05 mmol ml^{-1} and 20 mg ml^{-1}, respectively). The solution was heated to 90 °C in an oven for 15 min, followed by centrifugation. The separation efficiency (ϕ) of the water-soluble dyes was defined using the following equation:

$$\phi = \frac{C_0 - C_s}{C_0} \times 100\%$$

Here C_0 is the concentration of the dye in the initial solution and C_s is the concentration of the dye in the supernatant. Both C_0 and C_s could be determined from the UV-vis spectra.

2.4. Characterization

Fourier transform infrared spectra (FTIR). Fourier transform infrared spectra (FTIR) were recorded with a Paragon 1000 (Perkin-Elmer Co.). ^{1}H NMR measurements were carried out on a Varian Mercury Plus spectrometer operating at 400 MHz for protons equipped with a temperature control unit. $CDCl_3$ was used as solvent (TMS internal standard). Molecular weights (M_n) and molecular weight distributions (M_w/M_n) were determined by a PE Series 200 gel permeation chromatography (GPC). *N*,*N*-dimethylformamide (DMF) was used as the eluent at a flow rate of 1.0 mL min^{-1} and polystyrene as the calibration standard.

Transmission electron microscopy (TEM). A drop of the 1 g L^{-1} copolymer solution was placed onto a copper grid and excess solution was removed using filter paper. The sample was examined in a JEOL 2100F microscope, operating at 200 kV.

Cloud point (CP) measurement. The CPs of the polymer solutions were measured on a GBC Cintra 10e UV-visible spectrophotometer by monitoring the turbidity of the polymer solutions as a function of temperature at 550 nm and under a heating rate of 1 °C min^{-1}. The temperature at 90% light transmittance of the polymer solution was defined as the CP. The concentration of polymer used for CP determination was 3 g L^{-1}.

Dynamic light scattering (DLS). Dynamic light scattering studies of the copolymers at concentrations of 3 g L^{-1} were conducted using a Malvern Instruments Zetasizer Nano ZS instrument equipped with a 4 mW He–Ne laser (λ = 633 nm) at an angle of 90°, an avalanche photodiode detector with high quantum efficiency, and an ALV/LSE-5003 multiple τ digital correlator electronics system. The CONTIN analysis method was used.

Critical micelle concentration (CMC) measurements. The CMC of PDMS-gPEA was determined using Nile red as a fluorescent probe. Solutions of PDMS-gPEA with concentrations ranging from 1×10^{-4} to 1 g L^{-1} were prepared. The emission spectra were recorded using a LS-50B luminescence spectrometer (Perkin-Elmer Co.). The excitation wavelength was set at 559 nm. The fluorescence emission spectra were recorded between 580 nm and 750 nm. All fluorescence spectra were recorded at room temperature.

3. Results and discussion

3.1. Formation of PDMS-gPEA nanoparticles in aqueous solution

PDMS-gPEA was synthesized through condensation polymerization of commercially available poly(dimethylsiloxane) diglycidyl ether (PDMS-DE), poly(propylene glycol) diglycidyl

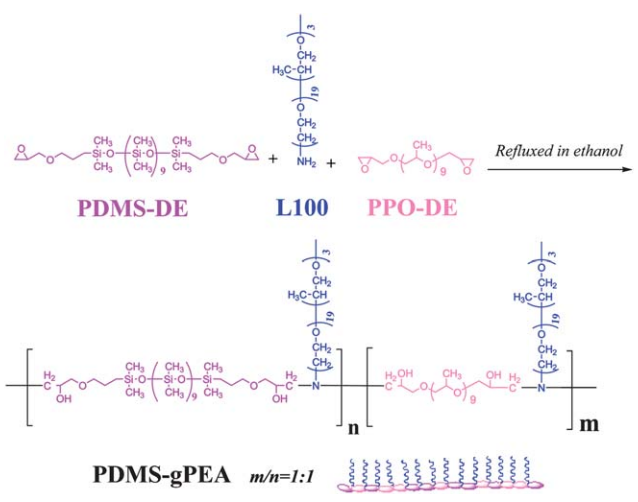

Scheme 1 The process for synthesis of PDMS-gPEA.

ether (PPO-DE) and Jeffamine L100. The process for synthesis of PDMS-gPEA is very simple, and is illustrated in Scheme 1. PDMS-gPEAs were designed based on the following rules. First, the poly(ether amine) chain was designed as the backbone, and L100 chains were introduced into the backbone as graft chains. Second, the PDMS in the backbone was designed as a hydrophobic part, which could lead to the formation of stable nanoparticles through self-assembly of PDMS-gPEA in aqueous solution, as the graft L100 chains were treated as hydrophilic parts. Third, L100 and PPO chains cause PDMS-gPEA to be responsive to temperature and ionic strength, while the amino group makes PDMS-gPEA respond to pH in aqueous solution. The successful synthesis of PDMS-gPEA was confirmed by FTIR, ^{1}H NMR and GPC. The details of FTIR, ^{1}H NMR and GPC are outlined in the ESI.†

The direct dispersion approach is a convenient and simple method, we therefore expected PDMS-gPEA to be directly dispersed in aqueous solution to form polymer nanoparticles (Scheme 2). The formation of polymer nanoparticles from PDMS-gPEA was verified by DLS and TEM (Fig. 1). DLS experiments were carried out in aqueous solution at 20 °C with a concentration of 3 g L^{-1}. DLS results indicated that PDMS-gPEA formed uniform-sized nanoparticles with diameters of about 16 nm (Fig. 1A). The sphere morphology of PDMS-gPEA was revealed by TEM imaging (Fig. 1B). Both DLS and TEM confirmed that PDMS-gPEA can self-assemble into polymer nanoparticles in aqueous solution through the approach of direct dispersion. To confirm self-assembly of amphiphilic polymers into polymer micelles, the critical micellization concentration (CMC) value for PDMS-gPEAs was determined by fluorescence spectroscopy, using Nile red as a probe. The relationship between the emission intensity of Nile red and the logarithm of PDMS-gPEA concentration was plotted. A sudden increase in emission intensity was observed at a concentration of about 5.2×10^{-2} g L^{-1} of PDMS-gPEA, indicating the onset of nanoparticle formation (Fig. 1C). The CMC value for PDMS-gPEA is one order of magnitude lower than that for gPEA (around 2.4×10^{-1} g L^{-1}),[40] indicating that the introduction of hydrophobic PDMS chains is a powerful method to reduce the CMC value of poly(ether amine). Polymer nanoparticles with lower CMC values are expected to be more stable when dispersed in water, which is important in practical applications.

3.2. Multi-responsive aggregation behavior of PDMS-gPEA nanoparticles

PDMS-gPEA nanoparticles were designed to respond to temperature, pH and ionic strength. PDMS-gPEA nanoparticles are composed of hydrophobic PDMS and PPO as their core and a hydrophilic part (L100) as the outer shell. The hydrophilic outer shell of L100 optimizes the surface contacting with water

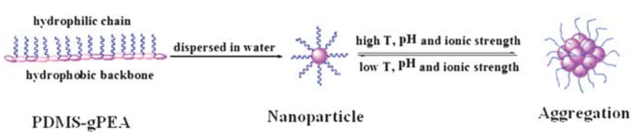

Scheme 2 The proposed process for formation and responsive aggregation of PDMS-gPEA nanoparticles.

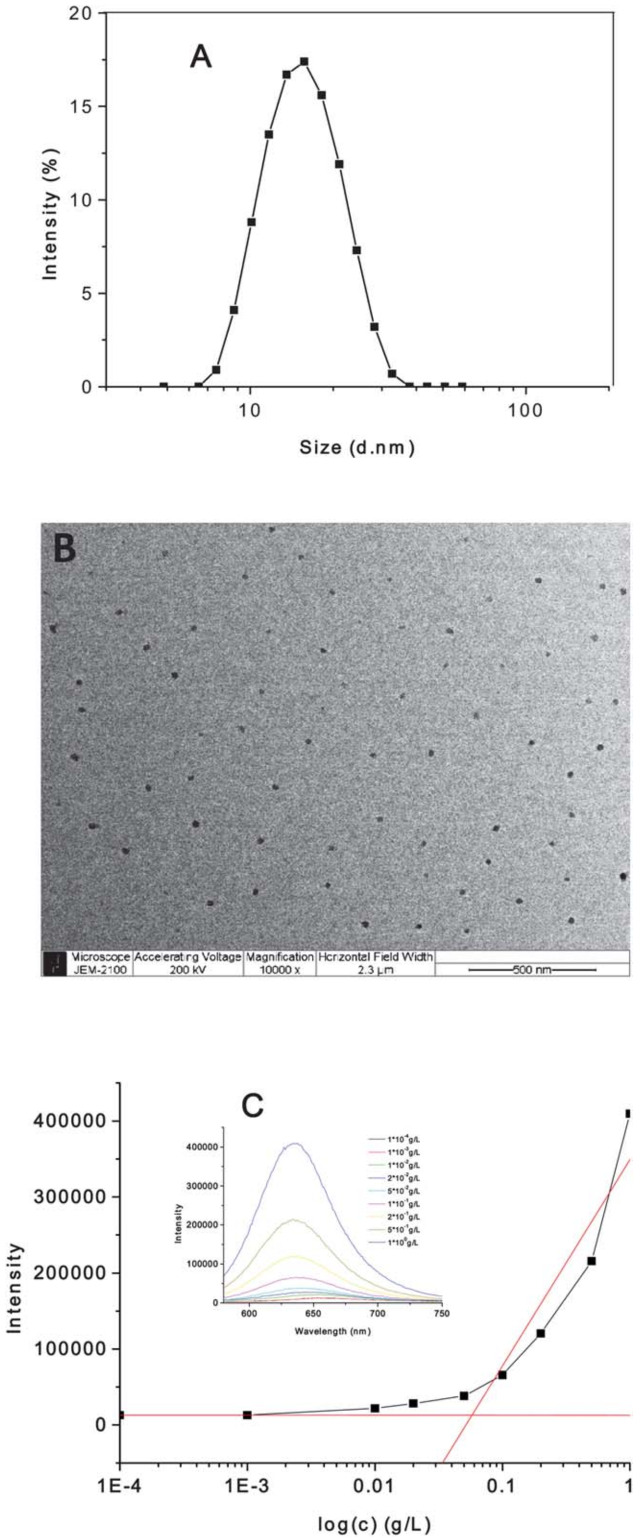

Fig. 1 A: The size distribution of PDMS-gPEA nanoparticles determined by DLS in aqueous solution (3 g L^{-1}) at 20 °C (PDI = 0.109); B: TEM images of PDMS-gPEA nanoparticles in aqueous solution at 20 °C; C: intensity of the fluorescence emission spectra of Nile red plotted *versus* PDMS-gPEA concentration. Inset: fluorescence emission of Nile red solution with different PDMS-gPEA concentrations.

and prevents the nanoparticle from aggregating further. With an increase in temperature, the hydrogen bonds between the water molecules and the hydrophilic part are destroyed. The outer shell becomes less hydrophilic, leading to the aggregation of PDMS-gPEA nanoparticles and the turbidity of the solution. The thermally responsive aggregation behavior of PDMS-gPEA nanoparticles under different conditions were investigated by measuring the cloud points. The concentration of PDMS-gPEA solutions were maintained at 3 g L^{-1} in all cases, which was much higher than the CMC to ensure the formation of polymer nanoparticles. A typical transmittance *vs.* temperature curve for PDMS-gPEA solution at pH = 7.0 is shown in Fig. 2A. The transparent PDMS-gPEA solution at room temperature suddenly became turbid when the temperature was above the CP, which can be seen visibly by photography. The turbid solution should result from the aggregation of PDMS-gPEA nanoparticles. The PDMS-gPEA solution exhibited a sharp response to temperature and the range of transition temperature was less than 1.5 °C. It should be noted that the thermally responsive aggregation of PDMS-gPEA nanoparticles is completely reversible (Fig. 2B).

To further understand the thermally responsive aggregation of PDMS-gPEA nanoparticles, DLS measurements were carried out to investigate the temperature dependence of the size distribution of PDMS-gPEA in aqueous solution at pH = 7.0 (Fig. 3). At temperatures below 63 °C, a single peak around 16–20 nm was observed, suggesting the PDMS-gPEA nanoparticles are stable and mantain a uniform size. With an increase of temperature to 65 °C, alongside the distribution at 16 nm, a new distribution above 1000 nm appears, indicating that the PDMS-gPEA nanoparticles start to aggregate to microparticles. These DLS results were in good agreement with the CP measurements. The behavior of the thermally responsive aggregation of PDMS-gPEA nanoparticles at high temperature (75 °C) was further investigated using TEM images (Fig. 4). Different morphologies of aggregation were observed in Fig. 4A,

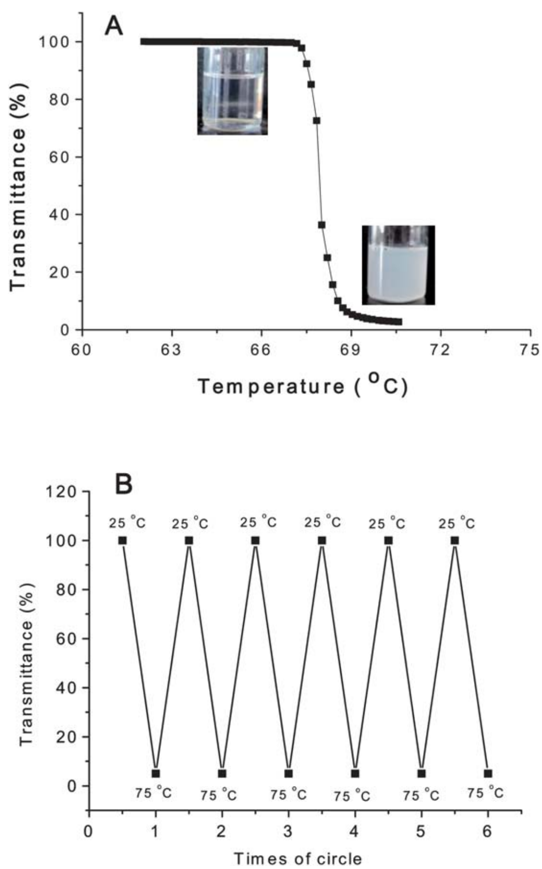

Fig. 2 A: The phase transition behavior of PDMS-gPEA aqueous solution (3 g L^{-1}) at pH = 7.0. Inset: photograph of PDMS-gPEA aqueous solution at low (25 °C) and high (75 °C) temperature; B: reversible change of transmittance of PDMS-gPEA aqueous solution between 25 °C and 75 °C.

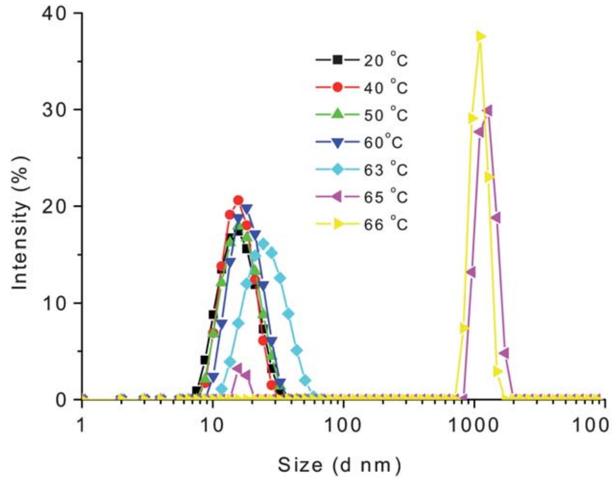

Fig. 3 Dynamic light scattering size distribution of PDMS-gPEA aqueous solution at different temperatures, pH = 7.0. (PDI: 20 °C = 0.109, 40 °C = 0.082, 50 °C = 0.112, 60 °C = 0.096, 63 °C = 0.113, 65 °C = 0.154, 66 °C = 1.000).

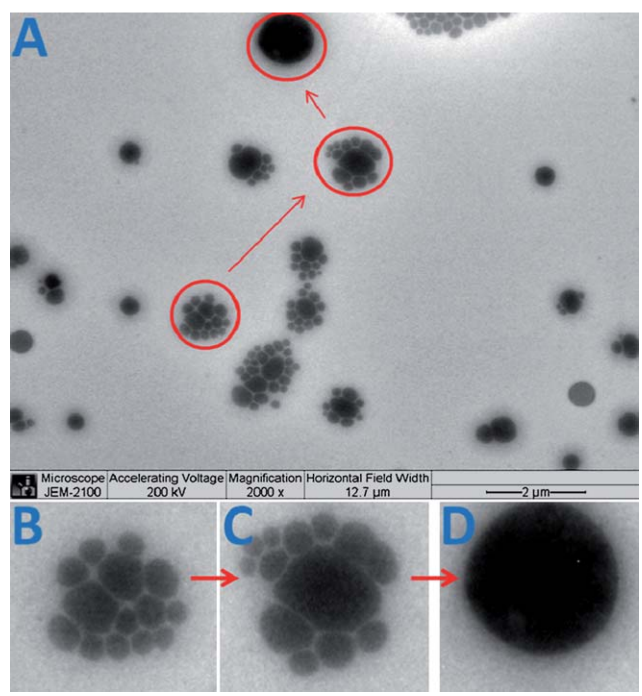

Fig. 4 TEM images of PDMS-gPEA in aqueous solution at high temperature (75 °C).

which are believed to be ascribed to different stages of aggregation. All PDMS-gPEA nanoparticles firstly aggregated into spherical particles with a size of more than 200 nm, which tended to aggregate (Fig. 4B and C). After fusion with each other, larger microparticles with sizes around 1000 nm were formed (Fig. 4D).

We also investigated the effect of pH and ionic strength on the aggregation of the PDMS-gPEA nanoparticles (Fig. 5). Fig. 5A shows the temperature dependence of transmittance for PDMS-gPEA aqueous solutions at different pH. The CP of PDMS-gPEA increased with a decrease in pH because the ternary amino groups were protonated at low pH. The protonated amino groups could improve the hydrophilicity of the outer shell of the PDMS-gPEA nanoparticles, resulting in aggregation at higher temperatures. Fig. 5B shows the transmittance *versus* temperature for SigPEA211 at different NaCl concentrations. Ionic strength is one of the dominating parameters in various aqueous systems, which has significant effects on the formation of hydrogen bonds between PEO and PPO chains and water molecules. PDMS-gPEA exhibited a very sharp phase transition over a wide range of NaCl concentrations. The CP decreased with increasing NaCl concentrations due to a typical salting-out effect.[43]

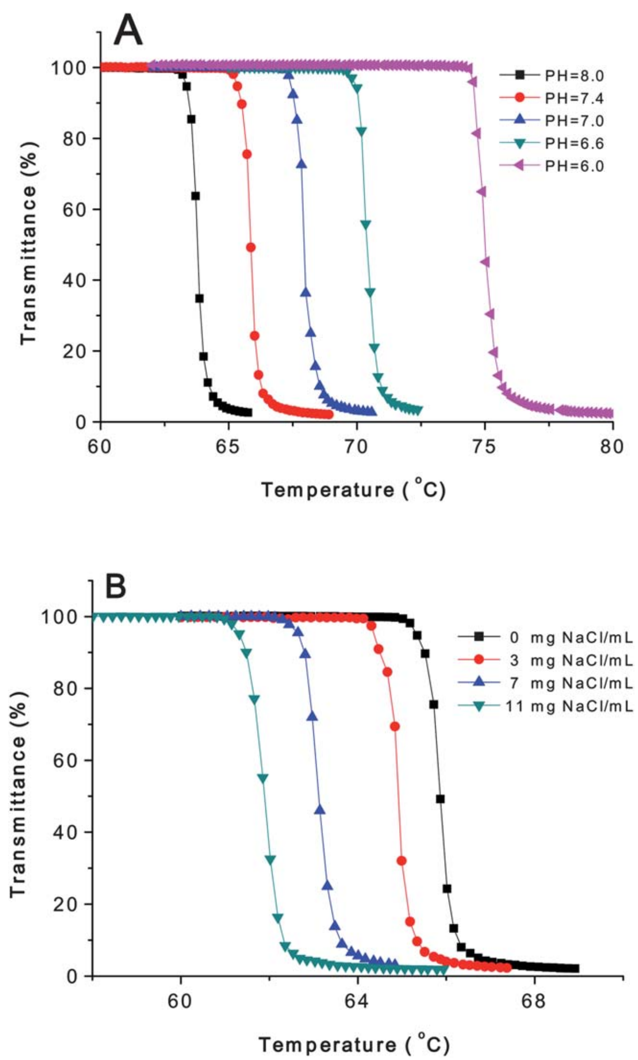

Fig. 5 The phase transition behavior of PDMS-gPEA aqueous solutions (3 g L^{-1}) at A: different pH and B: different ionic strengths (pH = 7.4).

3.3. Smart separation of dyes

Motivated by the novel characteristics of PDMS-gPEA such as easy synthesis, low cost and the ability to directly form polymer nanoparticles in aqueous solution with sharp multi-responses, we tried to develop a concept of smart separation and used PDMS-gPEA in the controlled separation of water-soluble dyes. Due to the response to external environmental stimulus, the structure of the hydrophobic core/hydrophilic shell and large surface areas, PDMS-gPEA nanoparticles are expected to encapsulate and adsorb some guest molecules selectively, then separate them by external environmental stimulus. At the same time, the interaction of the PDMS-gPEA nanoparticles with the guest molecules can help us further understand the responsive behavior. To confirm this idea, the water-soluble dye Rose Bengal (RB) was dissolved in a solution of PDMS-gPEA. The purple solution of RB and PDMS-gPEA possessed strong absorption at 561 nm (Fig. 6A and 7A) at room temperature. The purple solution of PDMS-gPEA and RB was heated to 90 °C (T > CP) and centrifuged. This produced deep purple precipitates at the bottom of tube, while the layer of solution above (supernatant) turned almost colorless (Fig. 6B). This could also be evidenced by the very weak absorption at 561 nm (Fig. 7A). It could be concluded that the RB molecules were sequestered as guest molecules by PDMS-gPEA nanoparticles in the water and precipitated with the PDMS-gPEA nanoparticles at high temperature (T > CP). We obtained the solution displayed in Fig. 6C by shaking the solution in Fig. 6B at room temperature (T < CP). The color of the solution returned to purple, indicating that the separation of RB was reversible and could be controlled using temperature.

To understand the interaction between RB and PDMS-gPEA nanoparticles, we compared the UV-vis absorption of RB in THF and in aqueous solution with and without PDMS-gPEA (Fig. 7A). It is notable that the maximum absorption wavelength (λ_{max}) of RB in aqueous solution red-shifted from 546 to 561 nm in the presence of PDMS-gPEA, which is close to RB absorption in medium polar THF solution. The obvious red-shifted λ_{max} of RB in the presence of PDMS-gPEA should be ascribed to the change in micro-environment of the RB in water, indicating that RB was sequestered as guest molecules into the hydrophobic core of the PDMS-gPEA nanoparticles. With an increase in temperature (T > CP), PDMS-gPEA nanoparticles which trapped RB tended to aggregate, resulting in precipitates of PDMS-gPEA

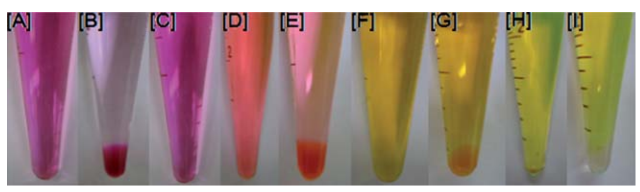

Fig. 6 Photograph of the separation of RB dye. A: solution of RB; B: solution of RB after separation; C: solution of recovered RB; D: solution of R6G; E: solution of R6G after separation; F: solution of MO; G: solution of MO after separation; H: solution of calcein; I: solution of calcein after separation.

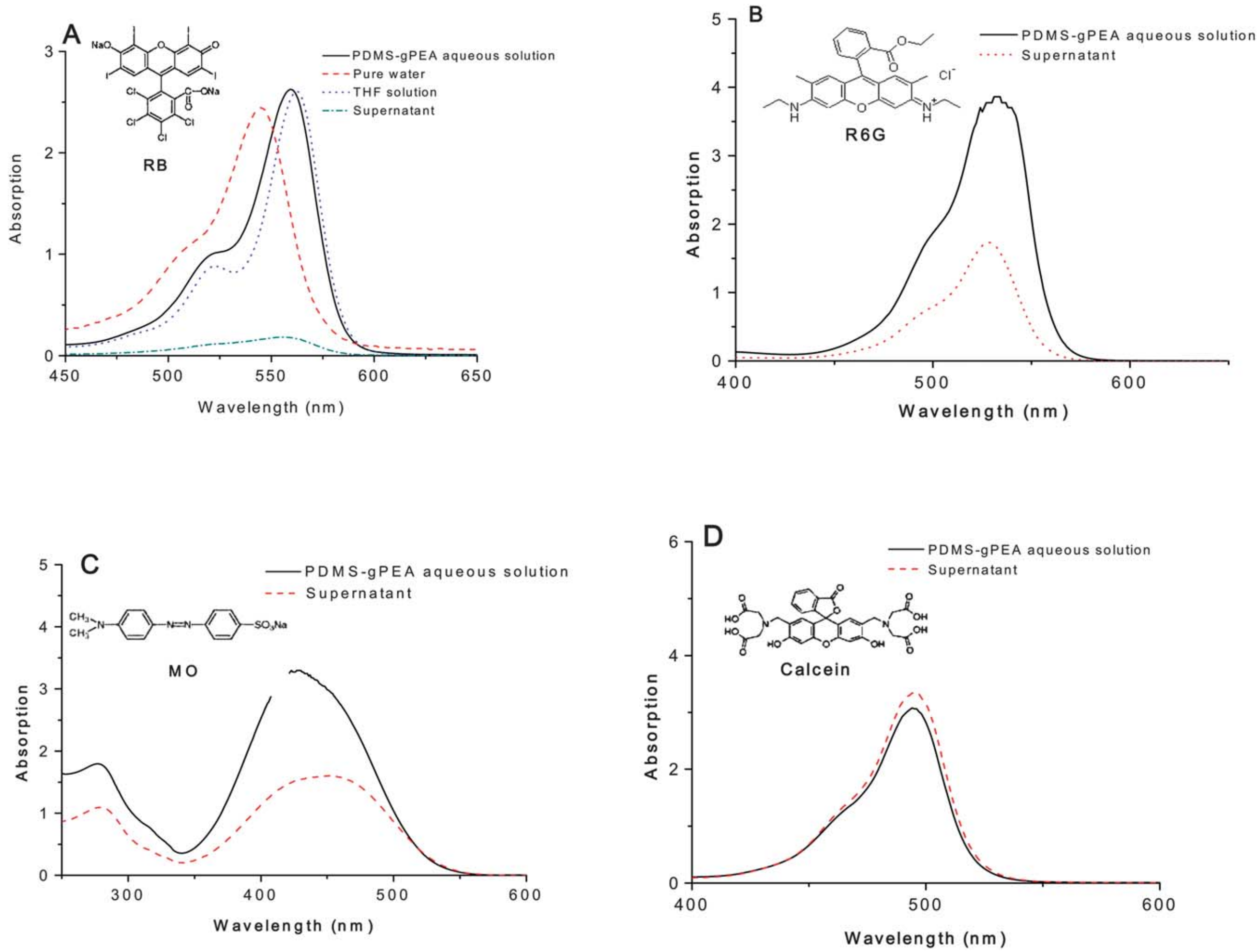

Fig. 7 UV-vis spectra of four water soluble dye solutions (A = Rose Bengal, B = Rhodamine 6G, C = MO, D = calcein) in separation experiment.

and separation of RB from water. This reversible separation of RB was driven and controlled by temperature.

To further understand the mechanism of the interaction between PDMS-gPEA nanoparticles and dye molecules, we also tried three other water-soluble dyes, Rhodamine 6G (R6G), methyl orange (MO) and calcein using the same method. The UV absorption of the dyes before and after separation triggered by temperature is shown in Fig. 7, and the related separation efficiency data is summarized in Fig. 8. The results showed that nearly half of the R6G and MO molecules were separated from water while none of the calcein molecules were separated from water. This can be seen in the photos in Fig. 6. Fig. 6D, F and H show the solutions of R6G, MO and calcein at low temperature

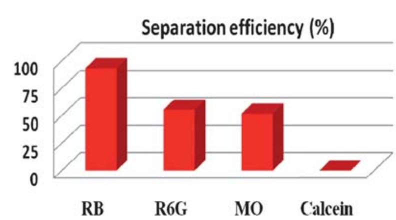

Fig. 8 Separation efficiency of four water-soluble dyes using PDMS-gPEA.

(T < CP), while Fig. 6E, G and I show the solutions of R6G, MO and calcein after separation. The color of the R6G and MO solutions after separation both became lighter and the precipitates seen in the bottom of tube displayed the color of R6G and MO, respectively, while the color of the calcein solution after separation remained green and the precipitates observed in the bottom of tube were colorless. Based on these results, PDMS-gPEA nanoparticles exhibited unique selective encapsulation of the guest dye molecules, which provides the possibility of selectively separating one kind of dye molecule from a mixture of different dyes.

To find the factors which determine this unique selectivity, more separation experiments using four other water soluble dyes were performed. Photographs and UV-vis spectra before and after separation are shown in Fig. S3.† The separation efficiencies of Amido black 10B (AB10B), alizarin yellow R (AYR), R Bordeaux red (BR) and neutral red (NR) were 63.9%, 70.4%, 43.2% and 74.2%, respectively. The reason that PDMS-gPEA nanoparticles could selectively encapsulate guest dye molecules is not completely clear yet. Taking the structure of the dyes and their separation efficiency into consideration, however, we propose two possible factors which determine selective encapsulation of guest dye molecules. First, the effect of the hydrophobicity of the dye should be the main driving force for

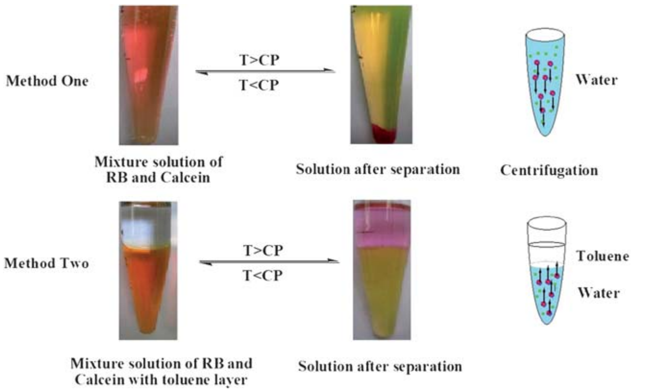

Fig. 9 Photograph of the selective separation of dye using PDMS-gPEA by two methods.

encapsulation. Stronger hydrophobicity of the dye could allow it to enter the core of PDMS-gPEA nanoparticle more easily, resulting in a higher separation efficiency. Second, electrostatic and van der Waals forces between the surface of the nanoparticles and the guest dye molecules lead to their binding to each other.

Taking advantage of the unique selective encapsulation of guest dye molecules, we could separate RB from a solution of RB and calcein in the presence of PDMS-gPEA. As shown in Fig. 9, RB could be separated from the solution of RB and calcein in two ways. The basic steps of the two methods were the same: the solution was heated to 90 °C (>CP), followed by centrifugation. The difference between the two methods was that toluene was added to the solution of RB and calcein in method two. The color of the aqueous solution of RB and calcein was orange. In method one, the color of solution after separation was yellow-green, like a calcein solution, and the color of the precipitates seen in the bottom of the tube was deep purple, the color of RB. This demonstrates the successful separation of RB from the solution of RB and calcein. In method two, a toluene layer was added above the solution of RB and calcein. At low temperatures, the toluene layer stayed transparent and colorless even if the tube was shaken for a while. Thayumanavan *et al.* have shown that polymer nanoparticles are stable in the solvent in which they are assembled, even in the presence of another immiscible, but favorable, solvents.[44,45] After being heated, shaken and centrifuged, the toluene layer turned purple and the water layer yellow-green, indicating that the RB and PDMS-gPEA have transferred into the toluene layer instead of precipitating at the bottom of tube. At high temperatures (T > CP), PDMS-gPEA may play a role (like a surfactant) in making RB disperse in a toluene layer. Instead of having any contact with water at high temperatures, PDMS-gPEA favored dispersal in the toluene layer. It should be noted that the separation of RB in both methods was reversible.

4. Conclusions

In summary, we developed a novel PDMS-containing amphiphilic poly(ether amine) (PDMS-gPEA), synthesized through one-pot condensation polymerization of commercial di-epoxy and amine monomers. The obtained PDMS-gPEA could directly self-assemble into stable uniform-sized nanoparticles in aqueous solution, whose aggregation could be controlled by temperature, pH and ionic strength. The responsive nanoparticles of PDMS-gPEA possessed the capacity for unique selective encapsulation of water-soluble dyes. Due to novel characteristics such as easy synthesis, low cost and the ability to self-assemble directly into polymer nanoparticles in aqueous solution, PDMS-gPEA is believed to have great potential in smart separations. In our lab, work continues to find the reasons for the selectivity.

Acknowledgements

We thank the National Nature Science Foundation of China (No. 50803036) and the Shanghai Leading Academic Discipline Project (No. B202) for their financial support.

References

1 D. E. Owens III, Y. C. Jian, J. E. Fang, B. V. Slaughter, Y. H. Chen and N. A. Peppas, *Macromolecules*, 2007, **40**, 7306–7310.
2 Y. F. Zhang, S. Z. Luo and S. Y. Liu, *Macromolecules*, 2005, **38**, 9813–9820.
3 N. Hantzschel, F. B. Zhang, F. Eckert, A. Pich and M. A. Winnik, *Langmuir*, 2007, **23**, 10793–10800.
4 R. K. O'Reilly, C. J. Hawker and K. L. Wooley, *Chem. Soc. Rev.*, 2006, **35**, 1068–1083.
5 C. Vancaeyzeele, V. Baranov, L. Shen, A. Abdelrahman and M. A. Winnik, *J. Am. Chem. Soc.*, 2007, **129**, 13653–13660.
6 A. Klaikherd, C. Nagamani and S. Thayumanavan, *J. Am. Chem. Soc.*, 2009, **131**, 4830–4838.
7 L. E. Bromberg and E. S. Ron, *Adv. Drug Delivery Rev.*, 1998, **31**, 197–221.
8 N. Willet, J. Gohy, L. Auvray, S. Varshney, R. Jérôme and B. Leyh, *Langmuir*, 2008, **24**, 3009–3015.
9 A. Kikuchi and T. Okano, *Prog. Polym. Sci.*, 2002, **27**, 1165–1193.
10 A. P. Goodwin, J. L. Mynar, Y. Ma, G. R. Fleming and J. M. J. Frechet, *J. Am. Chem. Soc.*, 2005, **127**, 9952–9953.
11 Y. Morishima, *Angew. Chem., Int. Ed.*, 2007, **46**, 1370–1372.
12 Q. Zhang, G. C. Clark, M. Wang, E. E. Remsen and K. L. Wooley, *Nano Lett.*, 2002, **2**, 1051–1054.
13 J. Jung, I.-H. Lee, E. Lee, J. Park and S. Jon, *Biomacromolecules*, 2007, **8**, 3401–3407.
14 B. Apostolovic and H. A. Klok, *Biomacromolecules*, 2008, **9**, 3173–3180.
15 C. Li, J. Madsen, S. P. Armes and A. L. Lewis, *Angew. Chem., Int. Ed.*, 2006, **45**, 3510–3513.
16 J. F. Mano, *Adv. Eng. Mater.*, 2008, **10**, 515–527.
17 J. L. Li, R. Bai and B. H. Chen, *Langmuir*, 2004, **20**, 6068–6070.
18 N. Rapoport, *Prog. Polym. Sci.*, 2007, **32**, 962–990.
19 P. S. Stayton, T. Shimoboji, C. Long, A. Chilkoti, G. H. Chen, J. M. Harris and A. S. Hoffman, *Nature*, 1995, **378**, 472–474.
20 T. Tang, V. Castelletto, P. Parras, I. W. Hamley, S. M. King, D. Roy, S. Perrier, R. Hoogenboom and U. S. Schubert, *Macromol. Chem. Phys.*, 2006, **207**, 1718–1726.
21 R. Hoogenboom, S. Rogers, A. Can, C. R. Becer, C. Guerrero-Sanchez, D. Wouters, S. Hoeppenera and U. S. Schubert, *Chem. Commun.*, 2009, 5582–5584.
22 S. L. Lin, X. H. He, Y. l. Li, J. P. Lin and T. Nose, *J. Phys. Chem. B*, 2009, **113**, 13926–13934.
23 J.-F. Lutz and A. Hoth, *Macromolecules*, 2006, **39**, 893–896.
24 Y. C. Wang, L. Y. Tang, Y. Li and J. Wang, *Biomacromolecules*, 2009, **10**, 66–73.
25 D. Cohn, G. Lando, A. Sosnik, S. Garty and A. Levi, *Biomaterials*, 2006, **27**, 1718–1727.
26 J.-F. Lutz, *J. Polym. Sci., Part A: Polym. Chem.*, 2008, **46**, 3459–3470.
27 S. L. Lin, N. Numasawa, T. Nose and J. P. Lin, *Macromolecules*, 2007, **40**, 1684–1692.
28 M. R. Xie, J. Y. Dang, H. J. Han, W. Z. Wang, J. W. Liu, X. H. He and Y. Q. Zhang, *Macromolecules*, 2008, **41**, 9004–9010.
29 Y. Z. You, C. Y. Hong, W. P. Wang, W. Q. Lu and C. Y. Pan, *Macromolecules*, 2004, **37**, 9761–9767.

30 G. D. Fu, S. J. Phua, E. T. Kang and G. H. Neoh, *Macromolecules*, 2005, **38**, 2612–2619.
31 F. Bougard, C. Giacomelli, L. Mespouille, R. Borsali, P. Dubois and R. Lazzaroni, *Langmuir*, 2008, **24**, 8272–8279.
32 N. A. Hadjiantoniou, T. Krasia-Christoforou, E. Loizou, P. Porcar and C. S. Patrickios, *Macromolecules*, 2010, **43**, 2713–2720.
33 B. S. Sumerlin, A. B. Lowe, D. B. Thomas and C. L. McCormick, *Macromolecules*, 2003, **36**, 5982–5987.
34 J. Adelsberger, A. Kulkarni, A. Jain, W. N. Wang, A. M. Bivigou-Koumba, P. Busch, V. Pipich, O. Holderer, T. Hellweg, A. Laschewsky, P. Muller-Buschbaum and C. M. Papadakis, *Macromolecules*, 2010, **43**, 2490–2501.
35 A. X. Mei, X. L. Guo, Y. W. Ding, X. H. Zhang, J. T. Xu, Z. Q. Fan and B. Y. Du, *Macromolecules*, 2010, **43**, 7312–7320.
36 O. G. Schramm, G. M. Pavlov, H. P. Erp, M. A. R. Meier, R. Hoogenboom and U. S. Schubert, *Macromolecules*, 2009, **42**, 1808–1816.
37 O. G. Schramm, M. A. R. Meier, R. Hoogenboom, H. P. van Erp, J.-F. Gohy and U. S. Schubert, *Soft Matter*, 2009, **5**, 1662–1667.
38 M. Motornov, Y. Roiter, I. Tokarev and S. Minko, *Prog. Polym. Sci.*, 2010, **35**, 174–211.
39 Y. R. Ren, X. S. Jiang and J. Yin, *J. Polym. Sci., Part A: Polym. Chem.*, 2009, **47**, 1292–1297.
40 Y. R. Ren, X. S. Jiang, R. Liu and J. Yin, *J. Polym. Sci., Part A: Polym. Chem.*, 2009, **47**, 6353–6361.
41 C. Cheng, K. T. Powell, E. Khoshdel and K. L. Wooley, *Macromolecules*, 2007, **40**, 7195–7207.
42 D. Neugebauer, Y. Zhang, T. Pakula and K. Matyjaszewski, *Macromolecules*, 2005, **38**, 8687–8693.
43 P. Alexandridis and J. F. Holzwarth, *Langmuir*, 1997, **13**, 6074–6082.
44 S. Basu, D. R. Vutukuri and S. Thayumanavan, *J. Am. Chem. Soc.*, 2005, **127**, 16794–16795.
45 T. S. Kale, A. Klaikherd, B. Popere and S. Thayumanavan, *Langmuir*, 2009, **25**, 9660–9670.